Correlated Spatiotemporal Evolution of Extreme-Ultraviolet Ribbons and Hard X-rays in a Solar Flare

By Stephen Naus, Jiong Qiu, Joel Dahlin, Richard DeVore, James Drake and Marc Swisdak

Overview

We study the structure and evolution of solar flare ribbons in the chromosphere to infer properties of magnetic reconnection that occurs in the corona. We analyze the imaging observations of the M7.3 SOL2014-04-18T13 flare obtained by IRIS in both the near and far ultraviolet (UV) passbands and by SDO/AIA in the 1600A passband. Two flare ribbons are observed to spread away from the magnetic polarity inversion line as the flare progresses. Using the high-resolution IRIS observations, we measure the width of the newly brightened ribbon front along the extension of the ribbon, which maps the feet of magnetic field lines reconnecting in the current sheet in the corona. We then compare the temporal evolution of the widths of the ribbon front with non-thermal hard X-ray (HXR) light curves at photon energies of 25-50 keV.

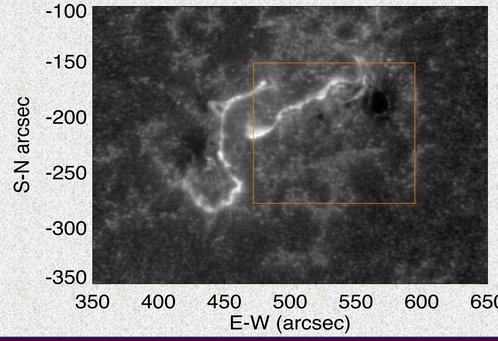

Left: Image of the M7.3 Flare SOL2014-04-18T13 in AIA1600 passband. The region outlined in orange is the area of IRIS observations with higher spatial resolution (0.17”/pixel).

Determination of the Ribbon Fronts

Left: IRIS2796 single pixel intensity profile. The horizontal lines indicate the threshold values chosen for three different ribbon front data sets as a multiple of the background (BG). The yellow rings show the time step that this pixel will be activated in the ribbon front data set.

Right: Histogram of the distribution of pixel intensity normalized to background at two separate times. There is a clear distinction between the flare (green) and non-flare (red) pixel distributions at those threshold values.

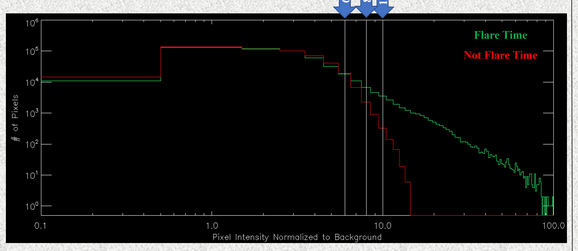

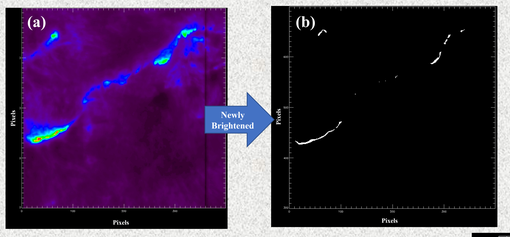

Panel a: IRIS2796 image of the M.7 flare during the rise phase.

Panel b: Ribbon front of the M.7 flare during the rise phase. This is constructed from the newly brightened (8x more than background) pixels in panel a.

Right: Temporal evolution of ribbon front pixels. The ribbon fronts at every three time steps (28s/time step) are shown. The color indicates the temporal evolution of the front. The field of view is divided into three separate regions: Regions 1, 2 & 3.

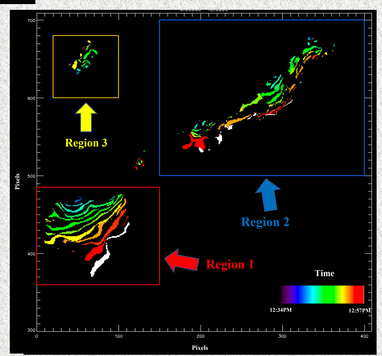

Hard X-ray and UV Light Curves

The light curves of Regions 1, 2, & 3 were compared with the HXR light curves from FERMI to determine where HXR emission is concentrated. The temporal evolution of the HXR emissions correlates strongly with the UV light curves in Region 1. On the other hand, in Regions 2 & 3 there was weak correlation between the UV and HXR light curves. This confirms that the HXR emissions come primarily from Region 1 (Brosius et al., 2016).

Bottom Left: Region 1 UV light curves with varying passbands and HXR light curve.
Bottom Right: Regions 2 & 3 UV and HXR light curves.

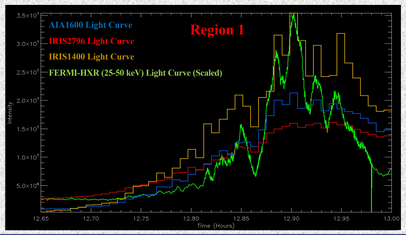

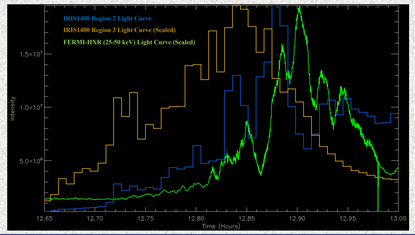

Measurement of Ribbon Front Widths

The perpendicular extent of the ribbon fronts in Regions 1 & 2 were measured at all time frames from t = 12:34 - 12:57 (UT). The shape of the ribbon is fitted to a curve. The localized width of the ribbon is defined as the number of pixels in a direction perpendicular to the curve at that location.

Bottom Left: Image of a ribbon front in Region 1 during the rise phase. The red line is the fitted curve along the ribbon front. The small blue markers indicate the location along the curve where the widths of the ribbon front are measured.
Bottom Right: The widths of the ribbon front (shown in the Bottom Left image) as a function of position along the ribbon in the x-direction.

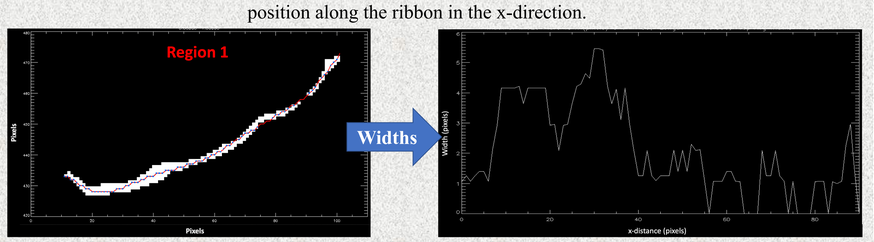

Results

Region 1 Widths

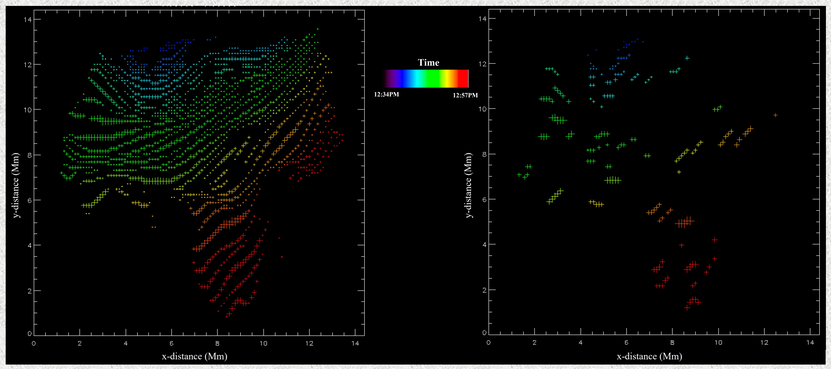

The width of the ribbon front is highly structured, possibly reflecting corresponding structure in the coronal reconnection region.

Top: Temporal evolution of the ribbons in Region 1. The symbol color indicates the time of brightening (see color bar). The symbol size is proportional to the width of the ribbon. *Left:* All locations at each time (8x BG). *Right:* Location of 5 largest widths at each time; note the patchy structure.

Right: The widths are displayed at all times. The color corresponds to the magnitude of the widths of the ribbon front at each location.

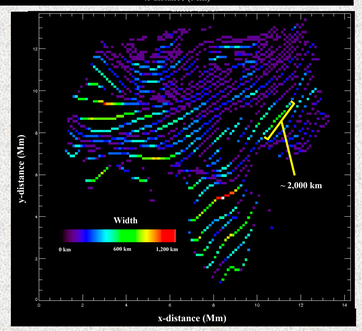

The widths of the ribbon fronts in Region 1 increase just prior to the HXR emission onset.

Right: The average of the top 5 widths at each time step are plotted alongside the HXR light curve.

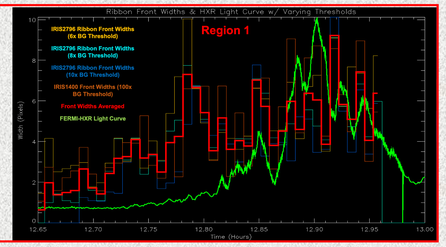

Region 2 Widths

There is weak correlation between the temporal evolution of the widths of the ribbon front in Region 2 and the HXR light curve.

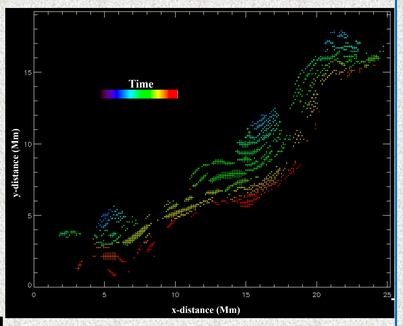

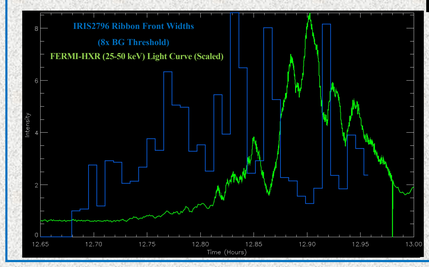

Top: Temporal evolution of the ribbons in Region 2 for all locations at each time. The symbol color indicates the time of brightening (see color bar). The symbol size is proportional to the width of the ribbon.

Left: The temporal evolution of the top 5 average widths at each time plotted alongside the HXR light curve.

Conclusion

- **Temporal evolution of UV flare ribbons and HXRs**
  - In Region 1, the FERMI-HXR light curves correlated strongly with the IRIS and SDO/AIA UV light curves. In addition, there is a strong relationship between the HXR emission and the measured widths of the flare ribbons.
  - In Regions 2 and 3, there was weak correlation between the HXR emission and the UV emission. There was little relationship between the HXR emission and ribbon widths in these regions.
  - Assuming the width of the ribbon fronts reflects the reconnection inflow speed at the coronal flare current sheet, our results suggest that there is a strong connection between the local reconnection rate and the non-thermal electron emission
- **Spatial structure of UV flare ribbons**
  - Ribbon fronts exhibited locally enhanced features of length 1.5-3 Mm along the ribbon and width 0.6-1.2 Mm perpendicular to the ribbon.
  - These widths agree with the results from the measurements using Goode Solar Telescope observations (Xu et al., 2016).
  - This highly structured nature of the ribbon fronts indicate that there may be similar structure in the reconnecting coronal flare current sheet

References

Brosius, et al., Astrophysical Journal, 830, 101, 2016

Xu, et al., Astrophysical Journal, 819, 89, 2016

Acknowledgments: This research was supported by the SOLFER DRIVE Center at UMD and by the OSTEM internship program at GSFC.